

Cite this: *Chem. Sci.*, 2024, 15, 3539

All publication charges for this article have been paid for by the Royal Society of Chemistry

Received 23rd November 2023

Accepted 24th January 2024

DOI: 10.1039/d3sc06280e

rsc.li/chemical-science

# Molecular imine cages with $\pi$ -basic $\text{Au}_3(\text{pyrazolate})$ faces†

Noga Eren, Farzaneh Fadaei-Tirani, Rosario Scopelliti and Kay Severin\*

One tetrahedral and two trigonal prismatic cages with  $\pi$ -basic  $\text{Au}_3(\text{pyrazolate})_3$  faces were obtained by connection of pre-formed gold complexes *via* dynamic covalent imine chemistry. The parallel arrangement of the  $\text{Au}_3(\text{pyrazolate})_3$  complexes in the prismatic cages augments the interaction with  $\pi$ -acids, as demonstrated by the encapsulation of polyhalogenated aromatic compounds. The tetrahedral cage was found to act as a potent receptor for fullerenes. The structures of the three cages, as well as the structures of adducts with  $\text{C}_{60}$  and  $\text{C}_{70}$ , could be established by X-ray crystallography.

## Introduction

Trinuclear gold complexes of the general formula  $\text{Au}_3(\text{pyrazolate})_3$  (Fig. 1a) were first described by Bonati and co-workers in 1974.<sup>1</sup> Following this initial report,  $\text{Au}_3(\text{pyrazolate})_3$  complexes were studied by numerous other groups.<sup>2</sup> These investigations have shown that  $\text{Au}_3(\text{pyrazolate})_3$  complexes display high chemical and thermal stability.<sup>2,3</sup> Similar to other Au(I) complexes,  $\text{Au}_3(\text{pyrazolate})_3$  trimers are prone to form Au...Au contacts in the solid state, and the presence of these aurophilic interactions is often associated with solid-state luminescence.<sup>2,4</sup> Luminescence can also be induced by the confinement of multiple  $\text{Au}_3(\text{pyrazolate})_3$  complexes in supramolecular hosts.<sup>5</sup> An important feature of  $\text{Au}_3(\text{pyrazolate})_3$  complexes is their variable  $\pi$ -acidity/basicity.<sup>2,6</sup> Most  $\text{Au}_3(\text{pyrazolate})_3$  complexes behave as  $\pi$ -bases.<sup>2,7</sup> However, the trimer  $\text{Au}_3[(3,5\text{-CF}_3)_2\text{pz}]_3$  was found to be  $\pi$ -acidic due to the presence of electron-withdrawing  $\text{CF}_3$  groups.<sup>8</sup>

$\text{Au}_3(\text{pyrazolate})_3$  complexes have found different applications.<sup>2</sup> For example, they were used to form mesogens,<sup>9</sup> stimuli-responsive organogels,<sup>10</sup> or conductive thin films.<sup>11</sup> Furthermore, a  $\text{Au}_3(\text{pyrazolate})_3$  complex was employed as a chemosensor for the selective detection of  $\text{Ag}^+$  ions,<sup>12</sup> and materials based on 2-dimensional nanosheets containing  $\text{Au}_3(\text{pyrazolate})_3$  complexes were used for photocatalytic hydrogen evolution.<sup>13</sup>

So far, there are few reports about cage-like structures with multiple  $\text{Au}_3(\text{pyrazolate})_3$  units. Thiel and co-workers have synthesized a hexanuclear Au complex, in which two  $\text{Au}_3(\text{pyrazolate})_3$  complexes are connected by three binaphthyl

spacers (Fig. 1b).<sup>14</sup> The complex was found to display poor solubility, preventing a solution-based characterization. Structurally related complexes with ferrocenyl linkers were described by Meyer and co-workers.<sup>15</sup> Again, poor solubility was encountered, hampering a more comprehensive characterization. The limited success in preparing defined complexes with multiple  $\text{Au}_3(\text{pyrazolate})_3$  units is in contrast to what was found for analogous  $\text{Cu}_3(\text{pyrazolate})_3$  and  $\text{Ag}_3(\text{pyrazolate})_3$  complexes.  $\text{Cu}_3(\text{pyrazolate})_3$  and  $\text{Ag}_3(\text{pyrazolate})_3$  complexes have been incorporated into prismatic and antiprismatic cages,<sup>16</sup> and some of these cages were found to encapsulate small molecules.<sup>16a-c</sup> Furthermore, there is a report about an octahedral cage containing four  $\text{Cu}_3(\text{pyrazolate})_3$  complexes,<sup>17</sup> and studies about bridged<sup>18</sup> or interlocked systems<sup>19</sup> with two  $\text{Cu}_3(\text{pyrazolate})_3$ -based prisms.

The difficulty in preparing more complex molecular structures with multiple  $\text{Au}_3(\text{pyrazolate})_3$  units is likely related to two features of  $\text{Au}_3(\text{pyrazolate})_3$  complexes. First, metallophilic interactions are stronger for  $\text{Au}_3(\text{pyrazolate})_3$  complexes than for analog  $\text{Cu}_3(\text{pyrazolate})_3$  and  $\text{Ag}_3(\text{pyrazolate})_3$  complexes.<sup>2</sup> Stronger intermolecular interaction can lead to reduced solubility. Second,  $\text{Au}_3(\text{pyrazolate})_3$  complexes are rather inert.<sup>20</sup> As a result, error correction processes are less efficient during

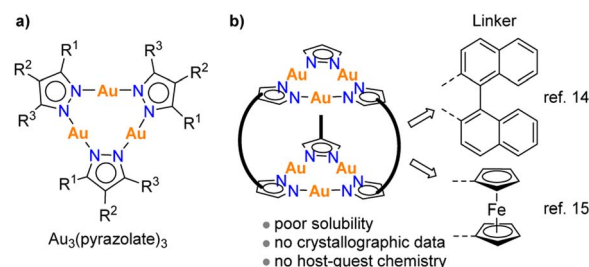


Fig. 1 The general structure of trinuclear gold pyrazolate complexes (a), and previously reported hexanuclear gold pyrazolate complexes with binaphthyl or ferrocenyl linkers (b).

Institut des Sciences et Ingénierie Chimiques, École Polytechnique Fédérale de Lausanne (EPFL), 1015 Lausanne, Switzerland. E-mail: kay.severin@epfl.ch

† Electronic supplementary information (ESI) available: Synthetic procedures and experimental details. CCDC 2284420–2284425 and 2309725. For ESI and crystallographic data in CIF or other electronic format see DOI: <https://doi.org/10.1039/d3sc06280e>

metallo-supramolecular syntheses. Notwithstanding these difficulties, we think that molecularly defined nanostructures with multiple  $\text{Au}_3(\text{pyrazolate})_3$  units are worthwhile synthetic targets, because the pronounced  $\pi$ -basicity of  $\text{Au}_3(\text{pyrazolate})_3$  complexes is expected to lead to interesting host properties.

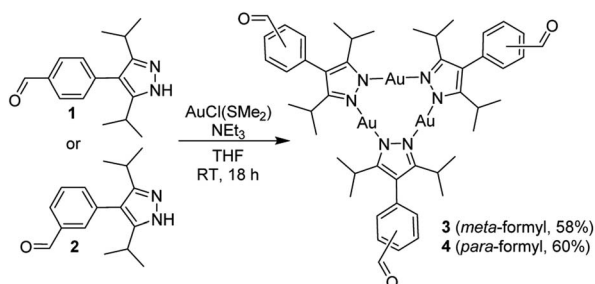
Below, we describe examples of well-soluble molecular cages containing two or four  $\text{Au}_3(\text{pyrazolate})_3$  faces. The cages were obtained by connection of pre-formed gold complexes *via* dynamic covalent imine chemistry. The presence of the Au complexes enables the molecular recognition of different guest molecules. Notably, a tetrahedral cage was found to be a potent receptor for  $\text{C}_{60}$  and  $\text{C}_{70}$ .

## Results and discussion

The substituted pyrazoles **1** and **2** (Scheme 1) were obtained by Suzuki cross-coupling reactions of 4-bromo-3,5-diisopropyl-1-tosyl-1*H*-pyrazole with the corresponding formylphenylboronic acids, followed by base-induced deprotection (for details, see the ESI<sup>†</sup>). Subsequent reactions with  $\text{AuCl}(\text{SMe}_2)$  in the presence of triethylamine in THF gave the  $\text{Au}_3(\text{pyrazolate})_3$  complexes **3** and **4** (Scheme 1). Both complexes are soluble in chloroform, but they display very poor solubility in acetonitrile and diethyl ether.

The trinuclear complexes **3** and **4** were characterized by NMR spectroscopy and single-crystal X-ray diffraction (XRD). The XRD analyses (Fig. 2) confirm that trinuclear complexes have formed.<sup>21</sup> In the solid state, **3** and **4** display a co-planar arrangement of the pyrazolate heterocycles, and the Au–N bond distances are within the expected range (1.98 to 2.02 Å). Close intermolecular Au...Au contacts are not observed.

Organic cages with imine linkages can be obtained in condensation reaction of di/poly-amines with di/poly-aldehydes.<sup>22</sup> The trinuclear complexes **3** and **4** appeared to be potentially well-suited for such condensation reactions.<sup>23</sup> However, the clean formation of imine cages is often not straightforward, even if the building blocks seem to have an appropriate geometry. Frequently encountered problems include incomplete condensation reactions, the formation of side products (insoluble polymers or mixtures of cages), and structural rearrangements during isolation.<sup>24</sup> In the following, we focus on reactions that resulted in the clean formation of a structurally defined cage. A brief discussion of reaction with other amines can be found in the ESI.<sup>†</sup>



Scheme 1 Synthesis of the complexes **3** and **4**.

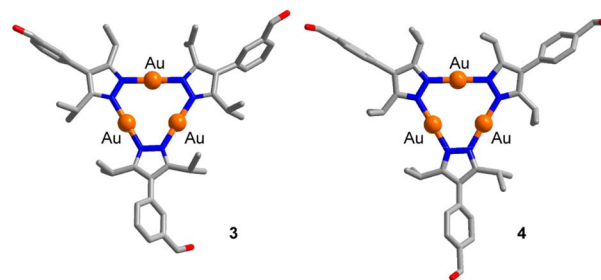
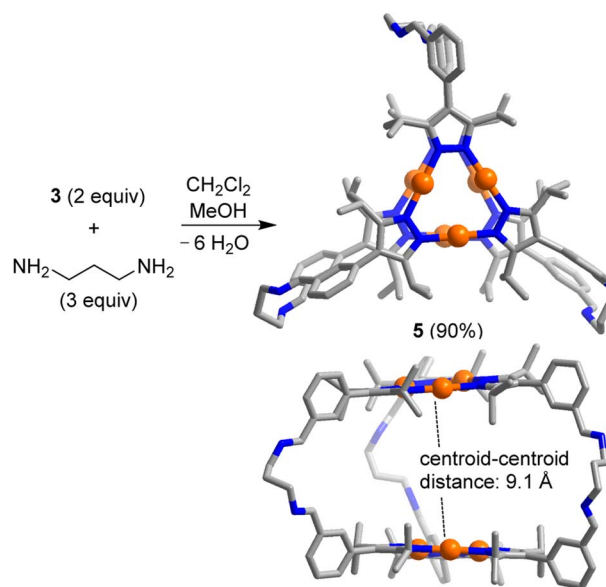


Fig. 2 Graphic representation of the molecular structures of **3** and **4** as determined by single-crystal XRD. Hydrogen atoms are not shown.

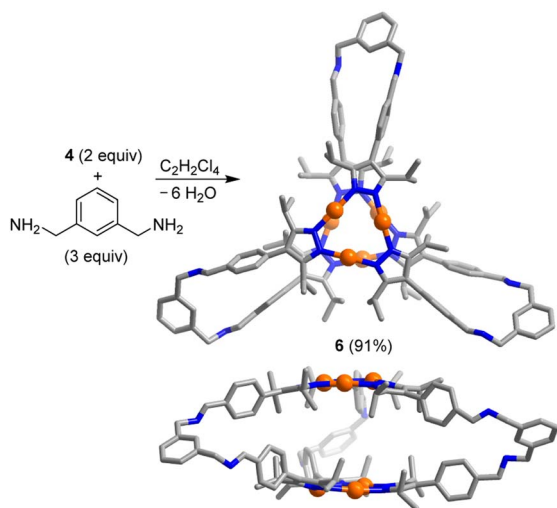
The reaction of complex **3** (2 equiv.) with 1,3-diaminopropane (3 equiv.) in a mixture of dichloromethane and methanol (3 : 2) gave the [2 + 3] condensation product **5** in high yield (Scheme 2). In solution, cage **5** displays high apparent symmetry, with only one set of NMR signals for the six bridging pyrazolate groups.

Single crystals of **5**, suitable for an XRD analysis, were obtained by layering of acetonitrile onto a solution of **5** in dichloromethane. The two  $\text{Au}_3(\text{pyrazolate})_3$  complexes in the trigonal prismatic cage **5** are arranged in a parallel fashion, with a distance between the planes of  $\sim 9$  Å and a distance between the centroids of 9.1 Å. This spacing suggests that **5** is potentially well-suited to bind 'flat' aromatic  $\pi$ -systems.<sup>2b</sup> The two Au trimers are roughly eclipsed with an angle of  $\sim 6^\circ$  between them.

The trigonal prismatic cage **6** was obtained in high yield by combining the Au trimer **4** with *m*-xylylenediamine in a ratio of 2 : 3 in  $\text{C}_2\text{H}_2\text{Cl}_4$  (Scheme 3). An XRD analysis of **6** revealed that the height of the prismatic cage, as defined by the distance between the planes of the Au trimers, is  $\sim 7$  Å. The overall size of prismatic **6** is significantly larger than that of **5**, with



Scheme 2 Synthesis of the prismatic cage **5**. The graphic representation of the product is based on a crystallographic analysis (view from the top and from the side; hydrogen atoms are not shown).

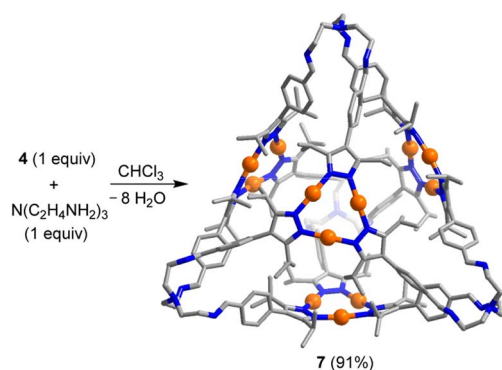


**Scheme 3** Synthesis of the prismatic cage **6**. The graphic representation of the product is based on a crystallographic analysis (view from the top and from the side; hydrogen atoms are not shown).

a maximum C...C distance of 26.8 Å (5: 20.4 Å). In contrast to what was found for **5**, one can observe short intermolecular Au...Au contacts in crystalline **6** (for details, see the ESI†). The deviation of the Au trimers from a staggered arrangement is  $\sim 25^\circ$ .

Tris(2-aminoethyl)amine (TREN) is frequently employed as a building block for the synthesis of imine-based organic cages.<sup>22a</sup> A mixture of TREN and the Au trimer **4** (ratio: 1 : 1) in CDCl<sub>3</sub> gave the [4 + 4] cage **7** (Scheme 4) in nearly quantitative yield as revealed by *in situ* NMR spectroscopy and ESI mass spectrometry analysis of the reaction mixture. Isolation of **7** was possible by precipitation with acetonitrile (yield: 91%).

At room temperature, the <sup>1</sup>H NMR spectrum of **7** in CDCl<sub>3</sub> showed very broad peaks for the CH signals of the phenylene groups. When cooling the solution to 273 K, four defined signals for the aromatic CH protons were observed. The underlying dynamic phenomenon is likely a hindered rotation of the tightly packed phenylene groups.<sup>23</sup> Another noteworthy



**Scheme 4** Synthesis of the tetrahedral cage **7**. The graphic representation of the product is based on a crystallographic analysis. Hydrogen atoms are not shown.

spectroscopic feature is the presence of two sets of NMR signals for iso-propyl substituents at the pyrazolate ligands. The appearance of two sets of signals is a consequence of the chirality of the TREN-based vertices,<sup>26</sup> rendering the iso-propyl groups diastereotopic.

A crystallographic analysis of **7** confirmed the tetrahedral shape of the cage (Scheme 4). The edge length of **7** is 24.8 Å (maximum C...C distance), making it one of the largest TREN-based imine cages described so far.<sup>22a</sup> The Au<sub>3</sub>(pyrazolate)<sub>3</sub> complexes panel the four faces of the tetrahedron. As deduced by NMR spectroscopy, the TREN-based vertices show a propeller-like conformation, with the same helical orientation for all four vertices. Residual electron density pointed to the presence of disordered solvent molecules. A solvent mask was calculated, and 2010 electrons were found in a volume of 7652 Å<sup>3</sup> in two voids per unit cell.<sup>27</sup> The solvent molecules, too disordered to be located in the electron density map, were taken into account using the Olex2 solvent-mask procedure.<sup>28</sup>

In crystalline **7**, close Au...Au contacts between the cages are observed (Fig. 3a). The corresponding Au...Au distances range from 3.268 to 3.393 Å. These auriphilic interactions are present for three out of the four Au<sub>3</sub>(pyrazolate)<sub>3</sub> complexes in cage **7**. To accommodate the Au...Au contacts, the Au<sub>3</sub>(pyrazolate)<sub>3</sub> complexes adopt a bent geometry (Fig. 3b), resulting in tetrahedral cages with slightly convex faces. A similar bending of the Au<sub>3</sub>(pyrazolate)<sub>3</sub> complexes was observed for the prismatic cage **6** (Scheme 3, graphic on the bottom). As discussed, this cage shows likewise intermolecular Au...Au contacts in the solid state.

The arrangement of the  $\pi$ -basic Au<sub>3</sub>(pyrazolate)<sub>3</sub> complexes in **5** and **6** suggested that the prismatic cages might be able to act as hosts for  $\pi$ -acidic aromatic compounds. This proposition could be corroborated by NMR studies. The addition of increasing amounts of octafluoronaphthalene to a solution of cage **5** in CD<sub>2</sub>Cl<sub>2</sub> resulted in complexation-induced shifts (CIS) of the <sup>1</sup>H NMR signals (for details, see the ESI†). The CIS *vs.* concentration data could be fitted to a 1 : 1 binding model resulting in an apparent association constant of  $K_a = 3.0 \pm 0.1 \times 10^2 \text{ M}^{-1}$  (Fig. S54†) (Scheme 5).

For cage **6**, the complexation of octafluoronaphthalene was found to be slow on the <sup>19</sup>F NMR time scale, and separate signals for the 'free' and the 'bound' guest were observed. By integration of the <sup>19</sup>F NMR signals, we were able to derive a binding constant of  $K_a = 6.8 \pm 0.7 \times 10^3 \text{ M}^{-1}$  (Fig. S50†). A similar value was

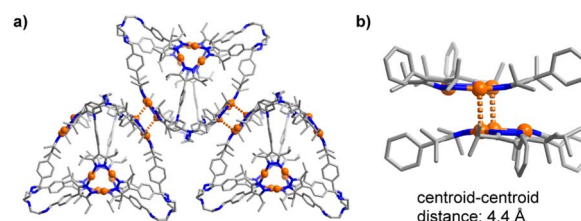
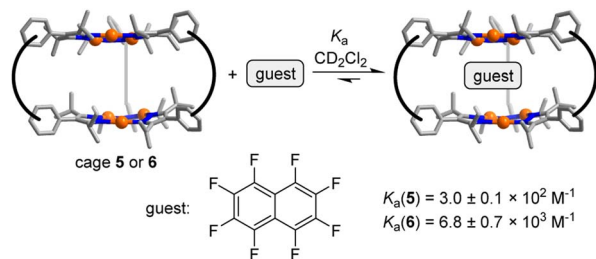


**Fig. 3** Auriphilic interactions between cages in crystalline **7** (a), and zoom-in on two Au<sub>3</sub>(pyrazolate)<sub>3</sub> complexes in **7**, highlighting the bent geometry of the trimers (b). Hydrogen atoms are not shown.





Scheme 5 Molecular recognition of octafluoronaphthalene.

derived from  $^1\text{H}$  NMR data (for details, see the ESI, Fig. S48 and S49†). The tighter binding of octafluoronaphthalene by cage 6 is possibly related to the reduced flexibility of the *m*-xylylene linkers when compared to the propylene linkers in cage 5. Hexabromobenzene and hexachlorobenzene are likewise bound by 5 and 6, as evidenced by NMR experiments (for details, see the ESI†). The parallel arrangement of the two  $\text{Au}_3(\text{pyrazolate})_3$  complexes in 5 and 6 is of key importance for the complexation of polyhalogenated compounds. In control experiments with the simple  $\text{Au}_3(\text{pyrazolate})_3$  complexes 3 and 4, we were not able to detect an interaction with polyhalogenated compounds.<sup>29</sup> Likewise, we were not able to observe a complexation of octafluoronaphthalene by cage 7.

Coinage metal pyrazolate complexes of the general formula  $[\text{M}\{3,5-(\text{CF}_3)_2\text{pz}\}]_3$  ( $\text{M} = \text{Cu}, \text{Ag}, \text{Au}$ ) were reported to form co-crystals with  $\text{C}_{60}$ , with four  $[\text{M}\{3,5-(\text{CF}_3)_2\text{pz}\}]_3$  complexes surrounding  $\text{C}_{60}$  in a tetrahedral fashion.<sup>30</sup> This finding inspired us to examine if cage 7 would be able to bind fullerenes.<sup>31</sup>

When  $\text{C}_{60}$  (2 equiv.) was added to a solution of cage 7 (1.7 mM) in  $\text{C}_2\text{D}_2\text{Cl}_4$ , the formation of the host-guest complex  $\text{C}_{60} \subset 7$  was detected by mass spectrometry. The complexation of  $\text{C}_{60}$  was found to be slow on the NMR time scale, and it could be monitored by  $^1\text{H}$  NMR spectroscopy. Quantitative formation of  $\text{C}_{60} \subset 7$  was observed within 12 h. Similar results were obtained with  $\text{C}_{70}$ . Upon mixing  $\text{C}_{70}$  and cage 7 in  $\text{C}_2\text{D}_2\text{Cl}_4$ , the adduct  $\text{C}_{70} \subset 7$  formed in quantitative yield as evidenced by  $^1\text{H}$  NMR spectroscopy and mass spectrometry. In competition experiments with equal amounts of  $\text{C}_{60}$  and  $\text{C}_{70}$ , we observed the formation of the adducts  $\text{C}_{60} \subset 7$  and  $\text{C}_{70} \subset 7$  in nearly equal amounts ( $\sim 10:8$ ).

The structures of  $\text{C}_{60} \subset 7$  and  $\text{C}_{70} \subset 7$  in the solid state were analyzed by single-crystal XRD. As expected, the fullerenes are

bound in the central cavity of cage 7 (Fig. 4). The distance between the fullerenes and the  $\text{Au}_3(\text{pyrazolate})_3$  complexes, as defined by the closest  $\text{Au} \cdots \text{C}$  contacts, is  $\sim 3.4 \text{ \AA}$ . The average distance between the centroids of the four  $\text{Au}$  trimers in  $\text{C}_{60} \subset 7$  is  $10.7 \text{ \AA}$ . For  $\text{C}_{70} \subset 7$ , the corresponding value is  $11.3 \text{ \AA}$  and for 7 it is  $11.8 \text{ \AA}$ . Intermolecular  $\text{Au} \cdots \text{Au}$  contacts, as observed for the 'empty' cage 7, are observed for  $\text{C}_{70} \subset 7$  but not for  $\text{C}_{60} \subset 7$  (for details, see the ESI†).

## Conclusions

Molecular cages containing  $\text{Au}_3(\text{pyrazolate})_3$  complexes were obtained by connection of pre-formed gold complexes *via* dynamic covalent imine chemistry. In contrast to previously described cages with  $\text{Au}_3(\text{pyrazolate})_3$  faces,<sup>14,15</sup> the imine cages are soluble in chlorinated organic solvents. It was therefore possible to perform solution-based analyses and to grow single crystals for XRD measurements. The parallel arrangement of the two  $\text{Au}_3(\text{pyrazolate})_3$  complexes in the trigonal prismatic cages 5 and 6 enabled the complexation of polyhalogenated aromatic compounds. Notably, we observed tight encapsulation of octafluoronaphthalene by cage 6 with an apparent binding constant of  $K_a = 6.8 \pm 0.7 \times 10^3 \text{ M}^{-1}$ . The tetrahedral cage 7 is able to form adducts with  $\text{C}_{60}$  and  $\text{C}_{70}$  in a competitive solvent such as tetrachloroethane. Overall, our results provide evidence that the incorporation of  $\text{Au}_3(\text{pyrazolate})_3$  complexes in molecularly defined nanostructures can give compounds with interesting host-guest chemistry.

## Data availability

The data that support the findings of this study are available in the ESI† of this article.

## Author contributions

N. E. and K. S. initiated the study, N. E. performed the experiments and analyzed the data, F. F.-T. and R. S. collected and processed the X-ray data, and N. E. and K. S. co-wrote the manuscript. All authors discussed the results and commented on the manuscript.

## Conflicts of interest

There are no conflicts to declare.

## Acknowledgements

The work was supported by the École Polytechnique Fédérale de Lausanne (EPFL).

## References

- 1 F. Bonati, G. Minghetti and G. Banditelli, *J. Chem. Soc., Chem. Commun.*, 1974, 88–89.
- 2 For review articles, see: (a) J. Zheng, Z. Lu, K. Wu, G.-H. Ning and D. Li, *Chem. Rev.*, 2020, **120**, 9675–9742; (b) R. Galassi,

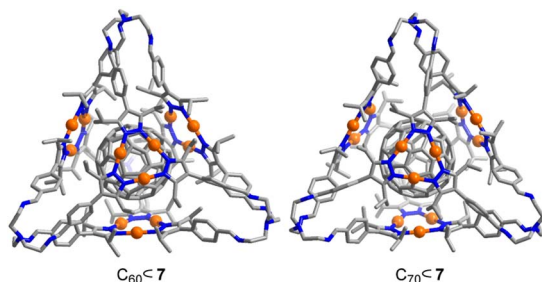


Fig. 4 Molecular structure of  $\text{C}_{60} \subset 7$  and  $\text{C}_{70} \subset 7$  as determined by single-crystal XRD. Hydrogen atoms are not shown.



- M. A. Rawashdeh-Omary, H. V. R. Dias and M. A. Omary, *Comments Inorg. Chem.*, 2019, **39**, 287–348; (c) J. Zheng, H. Yang, M. Xie and D. Li, *Chem. Commun.*, 2019, **55**, 7134–7146; (d) M. A. Omary, A. A. Mohamed, M. A. Rawashdeh-Omary and J. P. Fackler Jr, *Coord. Chem. Rev.*, 2005, **249**, 1372–1381; (e) A. Burini, A. A. Mohamed and J. P. Fackler, *Comments Inorg. Chem.*, 2003, **24**, 253–280.
- 3 G. Minghetti, G. Banditelli and F. Bonati, *Inorg. Chem.*, 1979, **18**, 658–663.
- 4 (a) Y. Kuroda, M. Tamaru, H. Nakasato, K. Nakamura, M. Nakata, K. Hisano, K. Fujisawa and O. Tsutsumi, *Commun. Chem.*, 2020, **3**, 139; (b) G. Yang and R. G. Raptis, *Inorg. Chem.*, 2003, **42**, 261–263.
- 5 M. Hanafusa, Y. Tsuchida, K. Matsumoto, K. Kondo and M. Yoshizawa, *Nat. Commun.*, 2020, **11**, 6061.
- 6 S. M. Tekarli, T. R. Cundari and M. A. Omary, *J. Am. Chem. Soc.*, 2008, **130**, 1669–1675.
- 7 Z. Lu, B. Chilukuri, C. Yang, A.-M. M. Rawashdeh, R. K. Arvapally, S. M. Tekarli, X. Wang, C. T. Cardenas, T. R. Cundari and M. A. Omary, *Chem. Sci.*, 2020, **11**, 11179–11188.
- 8 (a) R. Hahn, F. Bohle, S. Kotte, T. J. Keller, S.-S. Jester, A. Hansen, S. Grimme and B. Esser, *Chem. Sci.*, 2017, **9**, 3477–3483; (b) M. A. Omary, M. A. Rawashdeh-Omary, M. W. A. Gonser, O. Elbjeirami, T. Grimes and T. R. Cundari, *Inorg. Chem.*, 2005, **44**, 8200–8210.
- 9 (a) E. Beltrán, J. Barberá, J. L. Serrano, A. Elduque and R. Giménez, *Eur. J. Inorg. Chem.*, 2014, 1165–1173; (b) S. J. Kim, S. H. Kang, K.-M. Park, H. Kim, W.-C. Zin, M.-G. Choi and K. Kim, *Chem. Mater.*, 1998, **10**, 1889–1893; (c) J. Barberá, A. Elduque, R. Giménez, F. J. Lahoz, J. A. López, L. A. Oro and J. L. Serrano, *Inorg. Chem.*, 1998, **37**, 2960–2967; (d) J. Barberá, A. Elduque, R. Gimenez, L. A. Oro and J. L. Serrano, *Angew. Chem., Int. Ed. Engl.*, 1996, **35**, 2832–2835.
- 10 A. Kishimura, T. Yamashita and T. Aida, *J. Am. Chem. Soc.*, 2005, **127**, 179–183.
- 11 L. D. Earl, J. K. Nagle and M. O. Wolf, *Inorg. Chem.*, 2014, **53**, 7106–7117.
- 12 P. K. Upadhyay, S. B. Marpu, E. N. Benton, C. L. Williams, A. Telang and M. A. Omary, *Anal. Chem.*, 2018, **90**, 4999–5006.
- 13 X. Zhu, H. Miao, Y. Shan, G. Gao, Q. Gu, Q. Xiao and X. He, *Inorg. Chem.*, 2022, **61**, 13591–13599.
- 14 T. Jozak, Y. Sun, Y. Schmitt, S. Lebedkin, M. Kappes, M. Gerhards and W. R. Thiel, *Chem.-Eur. J.*, 2011, **17**, 3384–3389.
- 15 (a) M. Veronelli, S. Dechert, A. Schober, S. Demeshko and F. Meyer, *Eur. J. Inorg. Chem.*, 2017, 446–453; (b) M. Veronelli, S. Dechert, S. Demeshko and F. Meyer, *Inorg. Chem.*, 2015, **54**, 6917–6927.
- 16 (a) Z.-C. Shi, D.-X. Zhang, S.-Z. Zhan, M. Li, J. Zheng, H. Yang, X.-P. Zhou and D. Li, *Isr. J. Chem.*, 2019, **59**, 317–322; (b) L.-H. Li, J.-X. Zhang, S.-K. Jia and G. Yang, *Transition Met. Chem.*, 2016, **41**, 107–113; (c) P.-C. Duan, Z.-Y. Wang, J.-H. Chen, G. Yang and R. G. Raptis, *Dalton Trans.*, 2013, **42**, 14951–14954; (d) G.-F. Gao, M. Li, S.-Z. Zhan, Z. Lv, G.-h. Chen and D. Li, *Chem.-Eur. J.*, 2011, **17**, 4113–4117.
- 17 M. Grzywa, B. Bredenkötter, D. Denysenko, S. Spirkel, W. Nitek and D. Volkmer, *Z. Anorg. Allg. Chem.*, 2013, **639**, 1461–1471.
- 18 J.-H. Wang, M. Li, J. Zheng, X.-C. Huang and D. Li, *Chem. Commun.*, 2014, **50**, 9115–9118.
- 19 S.-Z. Zhan, J.-H. Li, G.-H. Zhang, X.-W. Liu, M. Li, J. Zheng, S. W. Ng and D. Li, *Chem. Commun.*, 2019, **55**, 11992–11995.
- 20 Ligand exchange processes for  $\text{Au}_3(\text{pyrazolate})_3$  complexes were found to be slow at room temperature.
- 21 For examples of tetranuclear  $\text{Au}_4(\text{pyrazolate})_4$  complexes, see: (a) R. A. Smith, R. Kulmaczewski and M. A. Halcrow, *Inorg. Chem.*, 2023, **62**, 9300–9305; (b) K. Fujisawa, Y. Ishikawa, Y. Miyashita and K.-i. Okamoto, *Inorg. Chim. Acta*, 2010, **363**, 2977–2989; (c) G. Yang and R. G. Raptis, *Inorg. Chim. Acta*, 2003, **352**, 98–104.
- 22 For reviews, see: (a) K. S. Gayen, T. Das and N. Chatterjee, *Eur. J. Org. Chem.*, 2021, 861–876; (b) K. Acharyya and P. S. Mukherjee, *Angew. Chem., Int. Ed.*, 2019, **58**, 8640–8653; (c) K. Ono and N. Iwasawa, *Chem.-Eur. J.*, 2018, **24**, 17856–17868; (d) M. Mastalerz, *Acc. Chem. Res.*, 2018, **51**, 2411–2422; (e) G. Zhang and M. Mastalerz, *Chem. Soc. Rev.*, 2014, **43**, 1934–1947; (f) N. M. Rue, J. Sun and R. Warmuth, *Isr. J. Chem.*, 2011, **51**, 743–768.
- 23 For the use of metal complexes with pendant aldehyde groups in imine cage synthesis, see: (a) L. S. Lisboa, D. Preston, C. J. McAdam, L. J. Wright, C. C. Hartinger and J. D. Crowley, *Angew. Chem., Int. Ed.*, 2022, **61**, e202201700; (b) L. S. Lisboa, J. A. Findlay, L. J. Wright, C. G. Hartinger and J. D. Crowley, *Angew. Chem., Int. Ed.*, 2020, **59**, 11101–11107; (c) C. Bravin, E. Badetti, F. A. Scaramuzza, G. Licini and C. Zonta, *J. Am. Chem. Soc.*, 2017, **139**, 6456–6460; (d) S. Bandi and D. K. Chand, *Chem.-Eur. J.*, 2016, **22**, 10330–10335; (e) H. Ding, X. Meng, X. Cui, Y. Yang, T. Zhou, C. Wang, M. Zeller and C. Wang, *Chem. Commun.*, 2014, **50**, 11162–11164; (f) A. Granzhan, C. Schouwey, T. Riis-Johannessen, R. Scopelliti and K. Severin, *J. Am. Chem. Soc.*, 2011, **133**, 7106–7115; (g) A. Granzhan, T. Riis-Johannessen, R. Scopelliti and K. Severin, *Angew. Chem., Int. Ed.*, 2010, **49**, 5115–5118.
- 24 A discussion of potential problems can be found in: T. Hasell and A. I. Cooper, *Nat. Rev. Mater.*, 2016, **1**, 16053.
- 25 T. Jiao, L. Chen, D. Yang, X. Li, G. Wu, P. Zeng, A. Zhou, Q. Yin, Y. Pan, B. Wu, X. Hong, X. Kong, V. M. Lynch, J. L. Sessler and H. Li, *Angew. Chem., Int. Ed.*, 2017, **56**, 14545–14550.
- 26 (a) T. Jiao, H. Qu, L. Tong, X. Cao and H. Li, *Angew. Chem., Int. Ed.*, 2021, **60**, 9852–9858; (b) W.-B. Gao, Z. Li, T. Tong, X. Dong, H. Qu, L. Yang, A. C.-H. Sue, Z.-Q. Tian and X.-Y. Cao, *J. Am. Chem. Soc.*, 2023, **145**, 17795–17804.
- 27 Porosity measurements were not performed because crystals of **7** were found to be very fragile.
- 28 O. V. Dolomanov, J. L. Bourhis, R. J. Gildea, J. A. K. Howard and H. Puschmann, *J. Appl. Crystallogr.*, 2009, **42**, 339–341.
- 29 For the highly  $\pi$ -basic  $\text{Au}_3(\text{bzim})_3$  ( $\text{bzim} = 1$ -benzylimidazole), an interaction with



- octafluoronaphthalene could be detected in solution. See: O. Elbjeirami, M. D. Rashdan, V. Nesterov and M. A. Rawashdeh-Omary, *Dalton Trans.*, 2010, **39**, 9465–9468.
- 30 N. B. Jayaratna, M. M. Olmstead, B. I. Kharisov and H. V. R. Dias, *Inorg. Chem.*, 2016, **55**, 8277–8280.
- 31 (a) X. Chang, Y. Xu and M. Von Delius, *Chem. Soc. Rev.*, 2024, **53**, 47–83; (b) C. Fuertes-Espinosa, M. Pujals and X. Ribas, *Chem*, 2020, **6**, 3219–3262; (c) C. García-Simón, M. Costas and X. Ribas, *Chem. Soc. Rev.*, 2016, **45**, 40–62; (d) D. Canevet, E. M. Pérez and N. Martín, *Angew. Chem., Int. Ed.*, 2011, **50**, 9248–9259.

